

# Substrate Integrated Waveguide Leaky-Wave Antenna With Wide Bandwidth via Prism Coupling

Lei Wang<sup>ID</sup>, Member, IEEE, José Luis Gómez-Tornero, Senior Member, IEEE,  
and Oscar Quevedo-Teruel, Senior Member, IEEE

**Abstract**—New communications systems require high-speed data transfer and need high frequency, wideband, and directive antennas. Leaky-wave antennas are a desirable type of antennas for millimeter and submillimeter waves, since they can produce a high directive radiation with a single feeding. The latter is an enormous advantage to reducing the cost and losses at high frequency. Despite these advantages, their dispersive nature inherently produces a beam squint effect in their radiation patterns. Here, we propose the use of a lens that compensates for the dispersion of the leaky wave, making the overall antenna broadband. This concept is demonstrated in substrate integrated waveguide technology at Ka-band, and the lens is integrated in the same technology. Full-wave simulations and experimental results are presented to demonstrate the potential of our proposal. Our manufactured prototype has more than 20% frequency bandwidth for the 3-dB pattern at  $\varphi = 31^\circ$ , and the main radiating direction steers only  $\pm 0.5^\circ$  from 35 to 40 GHz with a half-power beamwidth of  $8^\circ$ .

**Index Terms**—Dispersive lens, leaky-wave antennas (LWAs), metasurfaces, substrate integrated waveguide (SIW).

## I. INTRODUCTION

SUBSTRATE integrated waveguide leaky-wave antennas (SIW LWAs) offer interesting features for millimeter-wave wireless applications, since they offer high directivity and low losses using a single-feeding planar SIW guide [1]–[6]. As opposed to resonant antennas, their impedance bandwidth is wide due to their traveling-wave radiation mechanism, which is another general advantage of LWAs. However, due to their intrinsic dispersive nature [7], the directive radiated beam is scanned with frequency in all previous directive SIW LWA designs [1]–[7]. This is an important drawback for highly directive point-to-point broadband millimeter wireless links, since the pattern bandwidth (PBW) is very narrow due to this beam squinting. Actually, as the SIW LWA is more directive, the half-power beamwidth is narrower and the beam squint effect is more negative, reducing the effective bandwidth of

Manuscript received October 9, 2017; revised December 31, 2017; accepted March 15, 2018. Date of publication April 5, 2018; date of current version June 4, 2018. (Corresponding author: Lei Wang.)

L. Wang is with the Institute of Electromagnetic Theory, Hamburg University of Technology (TUHH), 21079 Hamburg, Germany (e-mail: wanglei@ieee.org).

J. L. Gómez-Tornero is with the Department of Communication and Information Technologies, Technical University of Cartagena, 30202 Cartagena, Spain (e-mail: jose.l.gomez@upct.es).

O. Quevedo-Teruel is with the Electromagnetic Engineering Laboratory, School of Electrical Engineering, KTH Royal Institute of Technology, SE-100 44 Stockholm, Sweden (e-mail: oscarqt@kth.se).

Color versions of one or more of the figures in this paper are available online at <http://ieeexplore.ieee.org>.

Digital Object Identifier 10.1109/TMTT.2018.2818149

directive, electrically long SIW LWAs for such fixed-angle applications.

As commonly done with wideband tapered slot antennas [8], [9] and wideband tapered microstrip LWAs [10], [11], SIW LWAs can be width-tapered [12]–[14] to make them broadband. However, this is at the cost of reducing their directivity. In fact, all width-tapered SIW LWA designs show broadened beams [15] or omnidirectional patterns [12]–[14]. As explained in [16] and [17], this drop in directivity results from the defocused radiation mechanism inherent to width-tapered LWAs. More recently, a coupled-SIW LWA topology has been proposed to reduce the beam squint effect [18], but again the main scanned beam is distorted due to the interference of coupled leaky modes which radiate simultaneously, thus losing directivity [19]. Another technique to increase the directive PBW uses a two-layer SIW LWA topology to synthesize a metamaterial response [20], thus losing the single layer simplicity of conventional SIW technology. Anisotropic [21], nonreciprocal [22], and active non-Foster circuits [23], [24] have been proposed to reduce the beam squint of directive LWAs. These solutions are complex, since they require biasing signals and expensive materials.

One fine solution of a high-gain scanned LWA with wide radiation PBW is the leaky lens proposed by Neto *et al.* in [25] and [26]. However, it has two important drawbacks. First, it is limited to a slot line printed between air and a dense dielectric, so that a nondispersive leaky mode radiates in the denser medium with a constant beam direction over a wide frequency band. Second, as a result of this form of radiation, this denser dielectric must be shaped to form a cylinder of elliptical cross sections of decreasing dimensions, so that the radiation can be eventually launched to free space. More recently, the addition of Huygens passive metasurfaces has been theoretically proposed in order to reduce the beam squint of general LWAs [27]. The main idea in [27] is that the LWA illuminates the metasurface, which introduces a complementary dispersive transmission response, which corrects for the beam squint of the dispersive LWA illuminator. Clearly, this type of solution is not limited to a nondispersive slot line like the leaky lens in [25], since this solution can theoretically be used to correct the beam squint of a dispersive leaky mode. However, no practical demonstration of this has been reported yet, probably due to the complexity of integrating this Huygens metasurface with a practical LWA.

In this paper, we propose a novel technique to obtain a directive squint-free SIW LWA, which dispenses from bulky

3-D-shaped dielectric lenses and integrates, in the same substrate, the LWA and a focusing lens with a prism shape. Leakage is obtained by separating the vias of one lateral wall of an SIW as proposed in [28] and [29]. This dispersive radiation of the SIW leaky mode is then absorbed by a prism made of vias, which is integrated in the same hosting substrate. The prism has a dispersive response that corrects for the beam squint of the SIW leaky mode. This integrated SIW structure is described in Section II, together with the theory to obtain a squint-free response. In Section III, an SIW antenna operating at 35 GHz is designed to radiate a directive narrow beam, with a constant scanning angle over a wideband. Section IV reports experiments on a fabricated prototype, and the main results are summarized in Section VI.

## II. MAIN ANALYSIS

### A. Principle of Operation

LWAs are known for their frequency-scanning properties, which are shown in Fig. 1(a). The electromagnetic waves inside the SIW travel in the  $y$ -axial direction, and the leaky waves radiate at a direction  $\varphi_L(f)$  that depends on the frequency. This effect is due to the inherent dispersive nature of the propagating mode in the waveguide. The propagation and the angle of radiation are defined as follows:

$$k_0^2 \times \epsilon_{r,L} = \beta_x^2 + \beta_y^2 \quad (1)$$

$$\sin \varphi_L(f) = \frac{\beta_y}{k_0 \times \sqrt{\epsilon_{r,L}}}. \quad (2)$$

It is well known that optical prisms made of a dispersive material can break up the light into different directions depending on the color. Each color represents a different frequency band. Equivalently, one can expect that these prisms can be used to focus frequency rays arriving from different directions to the same propagating direction. This idea is shown in Fig. 1(b), where the equivalent permittivity  $\epsilon_{r,P}(f)$  of the prism must be frequency-dependent, and it follows:

$$k_0^2 \times \epsilon_{r,P}(f) = \beta_x^2 + \beta_y^2 \quad (3)$$

$$\sin \varphi_P(f) = \frac{\beta_y}{k_0 \times \sqrt{\epsilon_{r,P}(f)}}. \quad (4)$$

If we place together a leaky-wave SIW and a dispersive prism,  $\beta_y$  must be linked in both structures defining a boundary condition

$$\beta_y = k_0 \times \sqrt{\epsilon_{r,L}} \times \sin \varphi_L(f) = k_0 \times \sqrt{\epsilon_{r,P}(f)} \times \sin \varphi_P(f) \quad (5)$$

and therefore

$$n_L \times \sin \varphi_L(f) = n_P(f) \times \sin \varphi_P(f). \quad (6)$$

This is exactly Snell's Law, where the equivalent refractive indexes are  $n_L = \sqrt{\epsilon_{r,L}}$  and  $n_P(f) = (\epsilon_{r,P}(f))^{1/2}$ . The refractive index  $n_L$  in the leaky-wave SIW is constant, whereas both the leaky-wave radiation direction  $\varphi_L(f)$  and the refractive index in the prism  $n_P(f)$  are frequency-dependent. Thus, to obtain a specific constant radiation direction  $\varphi_P(f)$

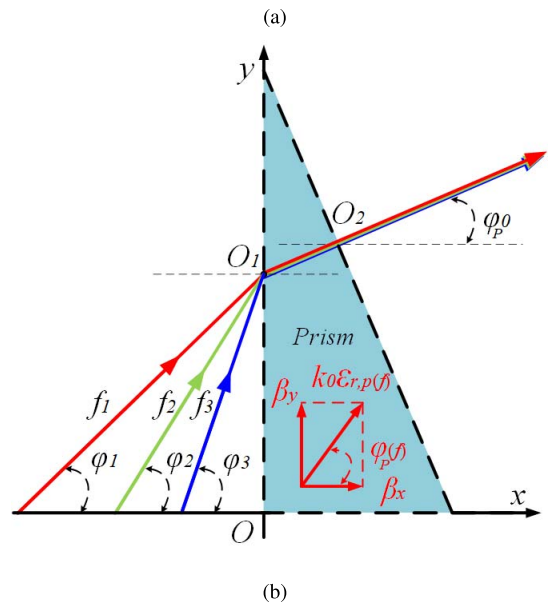
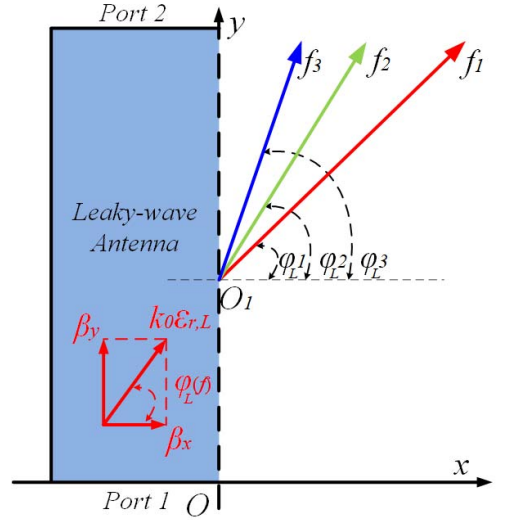


Fig. 1. Illustration of the proposed principle of operation. (a) Radiation angles in an LWA. (b) Combination of rays with different angular directions depending on the frequency by using a dispersive prism.

for a given leaky-wave characteristic  $\varphi_L(f)$ , the prism refractive index  $n_P(f)$  needs to be properly designed by

$$n_P(f) = \frac{n_L \times \sin \varphi_L(f)}{\sin \varphi_P(f)}. \quad (7)$$

### B. Dispersion Analysis

To analyze the dispersive characteristics of a leaky-wave SIW, a unit cell as shown in Fig. 2 (top) is modeled with periodic boundary conditions in the wave propagating direction with a periodicity of  $p_{\text{leaky}}$ . The radius  $r_{\text{via}}$  of the metallic vias is 0.15 mm, and the space between adjacent SIW vias is 0.5 mm. The width of the SIW (via center-to-via center) is 3.2 mm. By varying different values of  $p_{\text{leaky}}$  from 1.5 to 3.0 mm, four dispersion diagram curves are calculated and shown at the left side of lightline

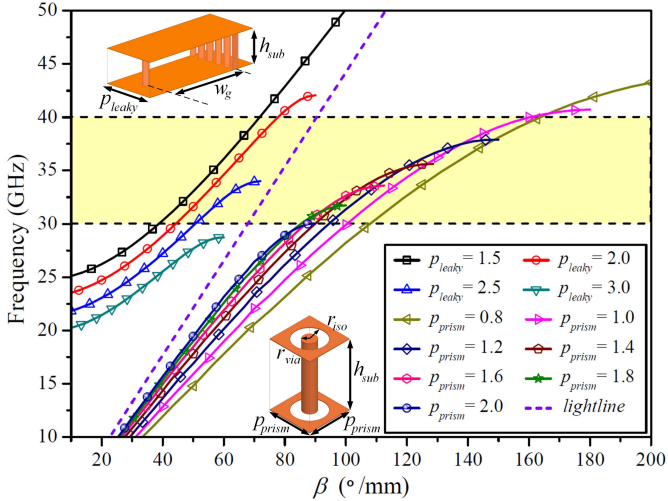


Fig. 2. Dispersion diagram of a number of leaky waveguides in an SIW with different periodicities  $p_{\text{leaky}}$  from 1.5 to 3.0 mm (left side). Dispersion of pins with periodicities  $p_{\text{prism}}$  from 0.8 to 2.0 mm (right side).

in Fig. 2. All these dispersion diagrams show the dispersive behavior of the original LWA.

The periodic structure as shown in Fig. 2 (bottom) has been selected for the design of the dispersive substrate integrated prism. It is a parallel metal-plate loading with an isolated metallic via. Its metallic via has the same radius  $r_{\text{via}}$  as the SIW, with the isolated circles of  $r_{\text{iso}} = 0.35$  mm on both the top and bottom plates. Several dispersion diagram curves are also shown at the right side of the lightline in Fig. 2, varying the periodicity  $p_{\text{prism}}$  from 0.8 to 2.0 mm.

Fig. 2 shows that these two kinds of dispersive curves are distributed at different sides of the lightline. The curves of the leaky-wave SIW go toward the lightline with the increase of propagation constant  $\beta$ , whereas the curves of the prism tend to go away from the lightline. It means that they feature two opposite dispersive characteristics, such as the curves of  $p_{\text{leaky}} = 1.5$  mm with  $p_{\text{prism}} = 0.8$  mm and  $p_{\text{leaky}} = 2.0$  mm with  $p_{\text{prism}} = 1.0$  mm. Therefore, combining the leaky-wave SIW and the dispersive prism, their dispersive characteristics can be compensated.

### C. Equivalent Refractive Index

From the dispersion diagram in Fig. 2, the equivalent refractive index  $n(f)$  can be calculated by

$$n(f) = \frac{\beta_y}{k_0}. \quad (8)$$

For the dispersive prism, the equivalent refractive index  $n_P(f)$  is frequency-dependent. The equivalent refractive index of the leaky-wave SIW  $n_L(f)$  is

$$n_L(f) = n_L \times \sin \varphi_L(f) \quad (9)$$

where  $n_L(f)$  is defined by the substrate permittivity  $\epsilon_r$ . Therefore,  $n_L(f)$  is always smaller than  $\sqrt{\epsilon_r}$ .

Fig. 3 shows both the equivalent refractive indexes of the dispersive prism and the leaky-wave SIW, with different

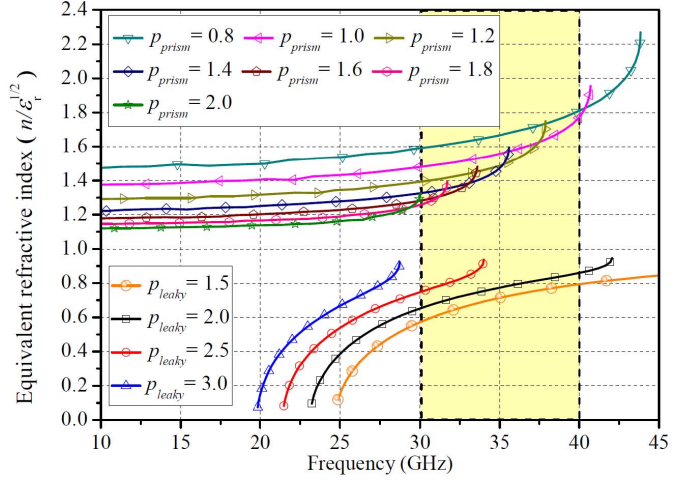


Fig. 3. Refractive index of pins and leaky waveguides presented in Fig. 2.

periodicities  $p_{\text{prism}}$  and  $p_{\text{leaky}}$ . Here, the shown equivalent refractive indexes have been normalized by the substrate permittivity factor  $\sqrt{\epsilon_r}$ . It can be found that the curve of the equivalent refractive index  $n_P(f)$  is concave with frequencies, whereas  $n_L(f)$  is convex.

### D. Radiation Direction

Taking (9) into (7), the radiation direction  $\varphi_P(f)$  can be deduced as

$$\varphi_P(f) = \arcsin \frac{n_L(f)}{n_P(f)} \quad (10)$$

where  $n_L(f)$  and  $n_P(f)$  can be obtained directly from Fig. 3 [30]. The black-square and golden-star curves in Fig. 4(a) and (b) show that the radiation directions have been corrected to be very constant between 30 and 40 GHz. For instance, the radiation direction of the curve with  $p_{\text{leaky}} = 2.0$  mm and  $p_{\text{prism}} = 1.0$  mm in Fig. 4(b) has a constant angle of  $28.5^\circ$ , with only  $\pm 0.5^\circ$  difference from 33 to 38.5 GHz. Fig. 4(c) and (d) shows that apart from the difference of the operating frequency, the dispersion correction is not as good as Fig. 4(a) and (b), which means that the dispersive prism must be designed *ad hoc* for a specific LWA.

## III. ANTENNA DESIGN

### A. Design of an LWA in SIW Technology

Aiming to design a weakly dispersive SIW LWA working between 30 and 40 GHz, only leaky-wave SIWs with a periodicity  $p_{\text{leaky}}$  of 1.5 and 2.0 mm are taken into consideration in the next steps. In leaky-wave SIWs with a periodicity  $p_{\text{leaky}}$  larger than 2.0 mm, the first mode does not propagate above 35 GHz, as shown in Figs. 2 and 3.

The selection of the leaky-wave periodicity  $p_{\text{leaky}}$  needs to take into consideration of both the operating frequency of the leaky-wave SIW and its leakage, which controls the radiation pattern. Fig. 5 shows the leakage parameter  $\alpha$  performance

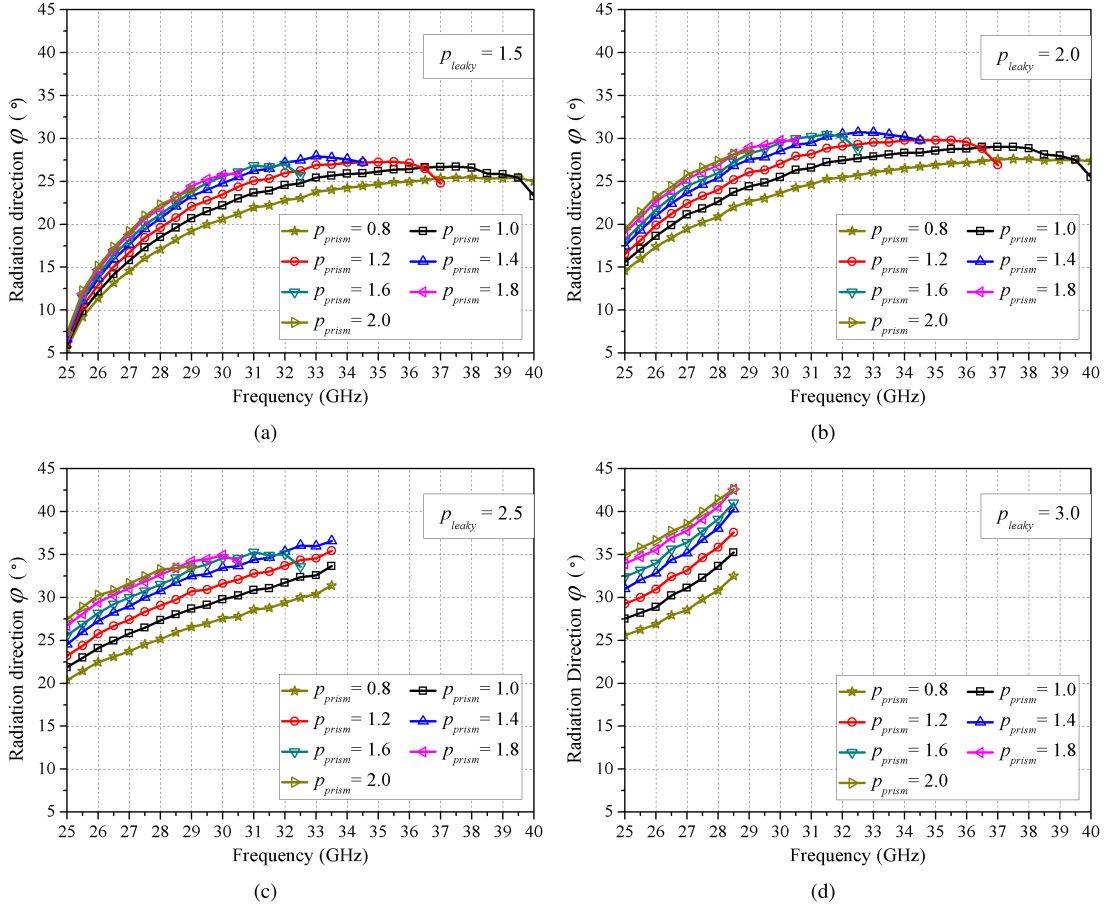


Fig. 4. Estimated radiation directions in the dispersive prism with different periodicities. (a)–(d) Different periodicities of the leaky-wave waveguide. (a)  $p_{\text{leaky}} = 1.5$  mm. (b)  $p_{\text{leaky}} = 2.0$  mm. (c)  $p_{\text{leaky}} = 2.5$  mm. (d)  $p_{\text{leaky}} = 3.0$  mm.

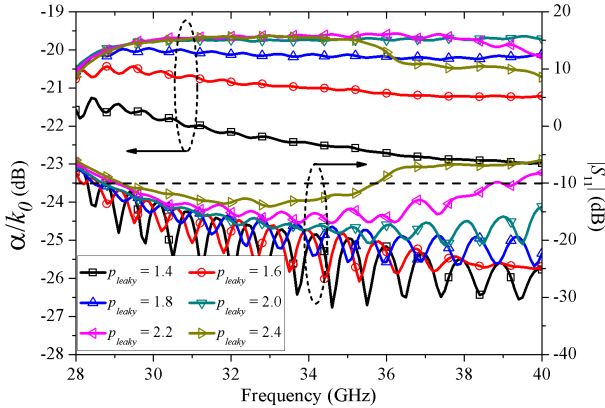


Fig. 5. Matching and amount of radiation leakage ( $\alpha$ ) for the LWAs with different periodicities.

in terms of the periodicity  $p_{\text{leaky}}$  and is approximately calculated by

$$\eta_{\text{rad}} = 1 - e^{-2\alpha L_A} = 1 - e^{-4\pi \frac{\alpha}{k_0} \frac{L_A}{\lambda_0}} \quad (11)$$

where  $L_A$  is the length of the leaky-wave SIW and  $\lambda_0$  is the free-space wavelength at the center frequency. Here, the leaky-wave SIW has a length chosen as  $L_A = 7\lambda_0$ . To avoid

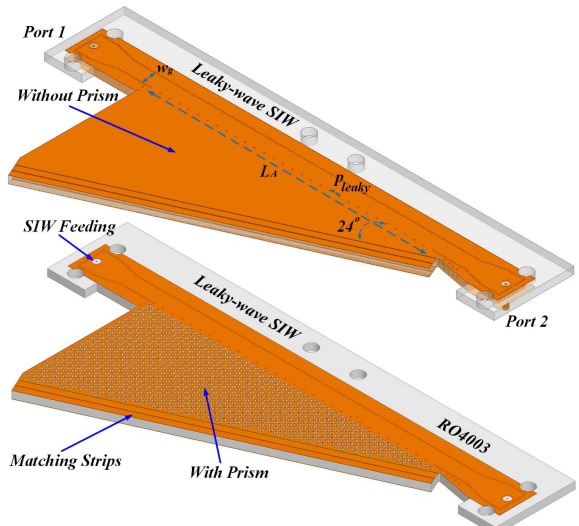


Fig. 6. Full structure of the proposed nondispersive leaky-wave SIW antenna, with and without a dispersive prism.

the reflection from the dielectric to the free space, a perfect matched layer boundary has been set up to calculate the leakage  $\alpha$ .

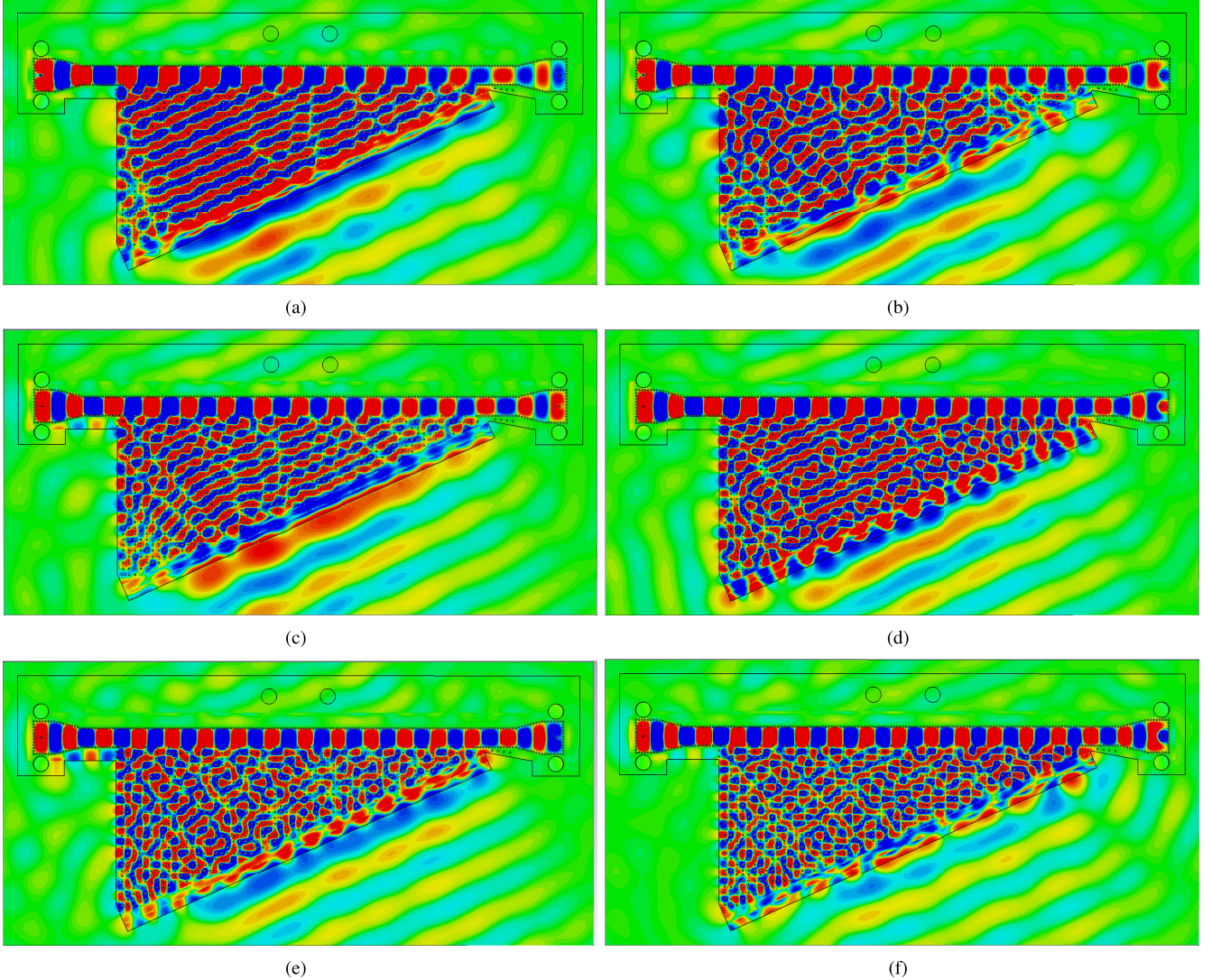


Fig. 7. Electric-field distribution for the proposed antenna for frequencies (a) 33, (b) 34, (c) 35, (d) 36, (e) 37, and (f) 38 GHz.

The SIW with a width of  $w_g = 3.2$  mm has a cutoff frequency of 27 GHz. Therefore, the performance of the antennas is analyzed from 28 to 40 GHz in Fig. 5. As expected, the leakage  $\alpha$  is higher when the periodicity  $p_{\text{leaky}}$  is larger, since a larger distance between pins allows larger radiation. When  $p_{\text{leaky}}$  is larger than 2.0 mm, the reflection coefficient starts to degrade due to a stronger mismatch. For all these reasons, a leaky-wave SIW with the parameters  $w_g = 3.2$  mm,  $L_A = 60$  mm, and  $p_{\text{leaky}} = 2.0$  mm has been chosen as a good compromise between the radiation and reflection coefficient.

#### B. Design of the Dispersive Prism

Since the leaky-wave SIW is designed with  $p_{\text{leaky}}$  of 2.0 mm, Fig. 4(b) will be used for design purposes. The angle of radiation and its frequency dependence can be modified with the substrate integrated prism. The prism with  $p_{\text{prism}}$  of 0.8 mm corrects the radiation direction to  $27^\circ$  with  $\pm 0.5^\circ$  difference from 34.5 to 40 GHz, whereas the

one with  $p_{\text{prism}}$  of 1.0 mm corrects the radiation direction to  $28.5^\circ$  with  $\pm 0.5^\circ$  difference from 33 to 38.5 GHz. The prism with  $p_{\text{prism}}$  of 1.0 mm is the preferred for our design, since it will provide a wider bandwidth.

In order to minimize the reflections and to maintain the angle of radiation, the substrate integrated prism has been cut with a triangular shape, as shown in Fig. 6. In this case, the radiation direction will be perpendicular to the prism boundary, as shown in Fig. 1(b).

#### C. Feeding Design

As utilized in [31], a 2.92-mm connector with a 1.524-mm probe pin has been used to feed the SIW. In addition, since the thickness of the material used, RO4003, is only 1.524 mm ( $\approx 0.18\lambda_0$ ), there will be a lot of reflections at the end of the parallel-plate waveguide. This strong mismatching can be solved by adding matching structures as in [32]. Two printed strips are added in front of the radiation aperture, as shown in Fig. 6.

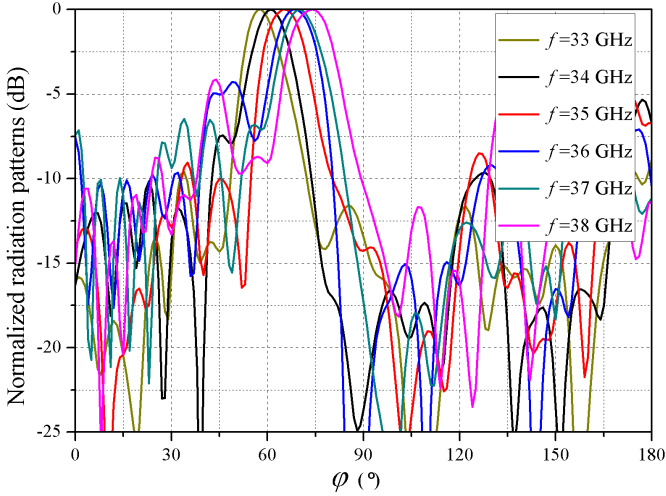


Fig. 8. Radiation patterns between 33 and 38 GHz for the antenna without the dispersive prism.

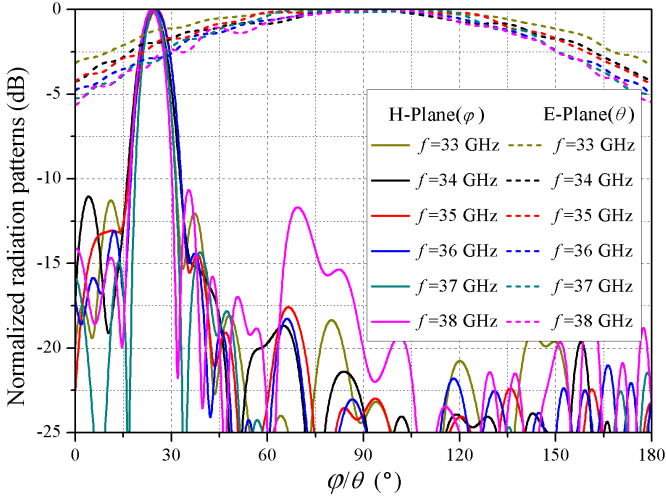


Fig. 9. Radiation patterns between 33 and 38 GHz for the antenna including the dispersive prism.

#### IV. SIMULATION RESULTS

##### A. Electric-Field Distribution

Considering the dimensions mentioned in Section III, the entire structure of our proposed nondispersive SIW LWA was built, including the leaky-wave SIW, dispersive prism, matching strips, and feeding, as shown in Fig. 6.

The electric-field at the frequency range between 33 and 38 GHz is calculated with a full-wave simulator and plotted in Fig. 7. As predicted, the electromagnetic waves at all these frequencies are leaking along the same direction, which is perpendicular to the designed prism boundary.

##### B. Weakly Dispersive Radiation

Fig. 8 shows the radiation patterns of the SIW leaky-wave without the substrate integrated prism, as shown in Fig. 6. This antenna has at least a 15° radiation beam steering from

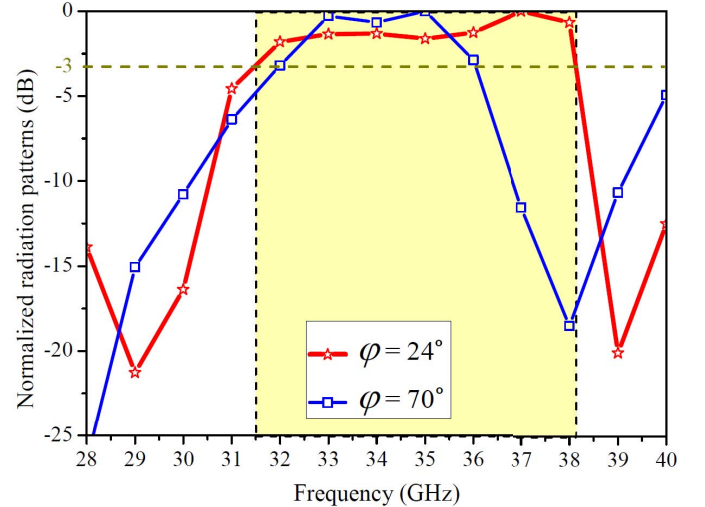


Fig. 10. Radiation level at a specific direction depending on the frequency. The case of 24° corresponds to the LWA with the dispersive prism, and the case of 70° is without prism.

33 to 38 GHz. However, when applying the prism as shown in Fig. 6, the radiation patterns radiate at  $\phi = 24^\circ$  with only  $\pm 0.5^\circ$  difference as shown in Fig. 9. The half-power beamwidth varies from  $8.0^\circ$  to  $9.0^\circ$  from 33 to 38 GHz, and the simulated sidelobe levels are all below  $-10$  dB. The radiation patterns in the *E*-plane at  $\phi = 24^\circ$  are also shown in Fig. 9. It can be observed the typical fan-beam radiation pattern of a thin, long aperture one-direction LWA as previously reported in [31]. As it is well known, the unwanted frequency beam squint is produced in the directive *H*-plane, and here, it is demonstrated the stabilization of the narrow beam direction in a wideband.

The achieved radiation direction  $\phi = 24^\circ$  is different from the one calculated theoretically, which was  $\phi = 28.5^\circ$ , as shown in Fig. 4(b). This difference is due to the coupling between the leaky-wave SIW and prism effects, which affects both the leakage  $\alpha$  and the radiation direction. This coupling can be controlled with the distance between both the structures. In our experience, this is a parameter that needs to be carefully optimized for designing this type of antenna.

The nondispersive performance can also be presented by the 3-dB radiation drop-off at a specific direction versus frequency, as shown in Fig. 10. Our proposed SIW LWA has a 3-dB gain drop-off from 31.5 to 38.2 GHz when radiating at  $\phi = 24^\circ$ , which means that the antenna has around 20% bandwidth when radiating at  $\phi = 24^\circ$ . For comparison purposes, Fig. 10 also shows the performances of the original SIW leaky-wave without a prism when radiating at  $\phi = 70^\circ$ . These results demonstrate the improvements in the bandwidth when applying a dispersive prism.

#### V. EXPERIMENT AND RESULTS

The proposed weakly dispersive SIW LWA has been manufactured in the RO4003 substrate with 1.524-mm thickness, as shown in Fig. 11. The antenna patterns are measured with one feeding port excited and the second port loaded with



Fig. 11. Prototype of the proposed leaky-wave SIW antenna and the measurement setup in the Antenna Laboratory at the KTH Royal Institute of Technology.

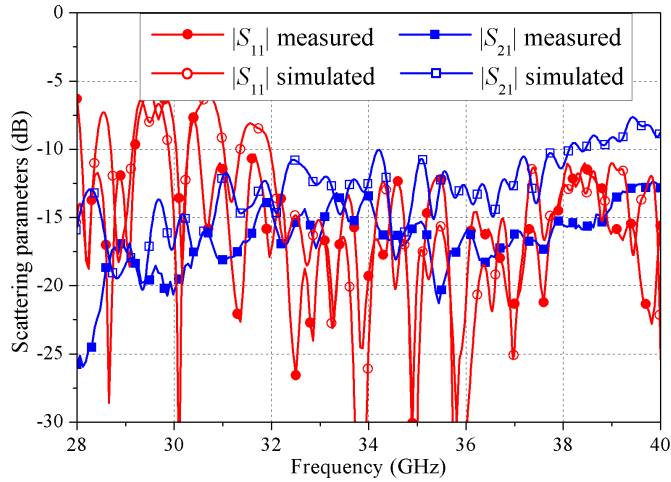


Fig. 12. Scattering parameters of the proposed LWA.

$50\ \Omega$  in the anechoic chamber at the KTH Royal Institute of Technology, as shown in Fig. 11.

#### A. Scattering Parameters

The simulated and measured  $S_{11}$  and  $S_{21}$  values are shown in Fig. 12. Our results show  $S_{11}$  below  $-10$  dB from 32 to 40 GHz. The simulated  $S_{21}$  value is also below  $-10$  dB from 32 to 36 dB, whereas it is higher than  $-10$  dB from 36.5 GHz. In our measurements,  $S_{21}$  is still beneath  $-10$  dB; however, there was a shift to higher frequencies.

#### B. Weakly Dispersive Radiation

Fig. 13 shows the measured radiation patterns of the proposed SIW LWA. It can be seen that the patterns from

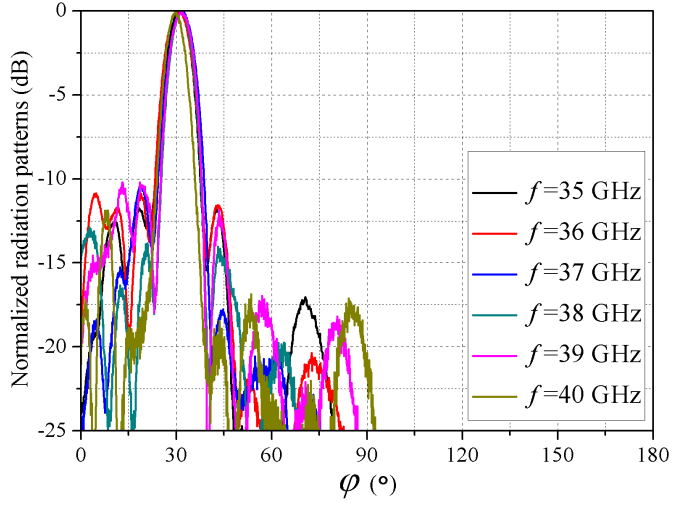


Fig. 13. Measured radiation patterns of the manufactured antenna.

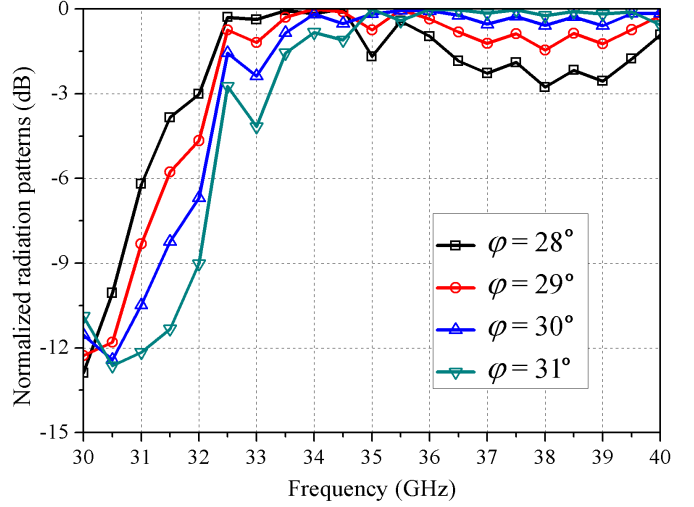


Fig. 14. Measured radiation levels at a specific direction as a function of the frequency.

35 to 40 GHz are all radiating at  $\varphi = 31^\circ$  with a  $\pm 0.5^\circ$  difference. The half-power beamwidth varies from  $8.0^\circ$  to  $9.0^\circ$ , and the sidelobe levels are lower than  $-10$  dB, which agree well with the simulation.

Fig. 14 shows the frequency bandwidth of 3-dB radiation drop-off at the direction of  $\varphi = 28^\circ$ ,  $29^\circ$ ,  $30^\circ$ , and  $31^\circ$ . It shows that the radiation at  $\varphi = 31^\circ$  does have less than 1-dB difference from 35 to 40 GHz and 3-dB difference from 33.2 to 40 GHz. For the direction of  $\varphi = 30^\circ$ , it has an even wider bandwidth from 34 to 40 GHz for 1-dB radiation difference and from 32.3 to 40 GHz ( $>21\%$ ) for 3-dB pattern difference.

#### C. Discussion About Differences Between Simulations and Measurements

There is a shift of the radiation direction from  $\varphi = 24^\circ$  to  $\varphi = 31^\circ$  between Figs. 9 and 13. After the further investigation of our structure, we have concluded that the prism is very

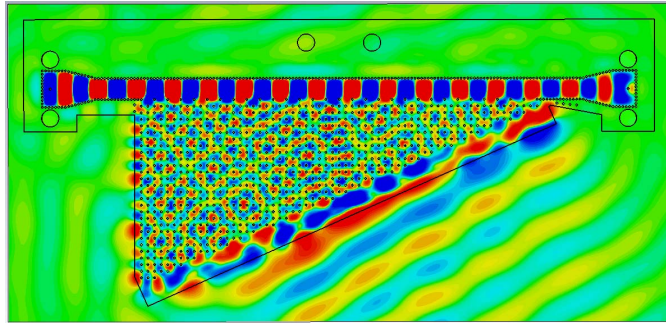


Fig. 15. Simulated electric field when  $r_{iso}$  is 0.4 mm instead of 0.35 mm.

sensitive to the parameter  $r_{iso}$  and is possibly causing the discrepancies. To illustrate this effect, a simulation has been done by changing  $r_{iso}$  from 0.35 to 0.4 mm. As a result, the radiation direction exactly shifts from  $24^\circ$  to  $31^\circ$ , as represented in Fig. 15. With this minor change, the operating frequency also shifts from 33 to 38 GHz to higher frequencies, 34–40 GHz, together with better leakage performance ( $S_{21}$ ) around 39 GHz, which is the exact effect that we experienced in our measured  $S_{21}$ , as represented in Fig. 12.

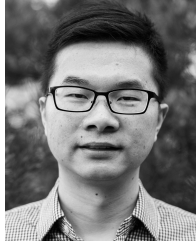
## VI. CONCLUSION

A weakly dispersive SIW LWA based on the use of a prism has been proposed, designed, and experimentally validated. Both simulation and experiment show that the proposed LWA has more than 20% frequency bandwidth for 3-dB pattern at the specific direction of  $\varphi = 31^\circ$ . The radiation directions steer only  $\pm 0.5^\circ$  from 35 to 40 GHz, with a narrow half-power beamwidth of  $8^\circ$ . Our weakly dispersive SIW LWA overcomes the conventional problem of squint effect. Our results extend the use of LWAs for applications in which a wideband radiation directed at a fixed angle is required.

## REFERENCES

- [1] F. Xu and K. Wu, "Guided-wave and leakage characteristics of substrate integrated waveguide," *IEEE Trans. Microw. Theory Techn.*, vol. 53, no. 1, pp. 66–73, Jan. 2005.
- [2] J. Xu, W. Hong, H. Tang, Z. Kuai, and K. Wu, "Half-mode substrate integrated waveguide (HMSIW) leaky-wave antenna for millimeter-wave applications," *IEEE Antennas Wireless Propag. Lett.*, vol. 7, pp. 85–88, Apr. 2008.
- [3] Y. J. Cheng, W. Hong, and K. Wu, "Millimeter-wave half mode substrate integrated waveguide frequency scanning antenna with quadri-polarization," *IEEE Trans. Antennas Propag.*, vol. 58, no. 6, pp. 1848–1855, Jun. 2010.
- [4] F. Xu, K. Wu, and X. Zhang, "Periodic leaky-wave antenna for millimeter wave applications based on substrate integrated waveguide," *IEEE Trans. Antennas Propag.*, vol. 58, no. 2, pp. 340–347, Feb. 2010.
- [5] Y. J. Cheng, W. Hong, K. Wu, and Y. Fan, "Millimeter-wave substrate integrated waveguide long slot leaky-wave antennas and two-dimensional multibeam applications," *IEEE Trans. Antennas Propag.*, vol. 59, no. 1, pp. 40–47, Jan. 2011.
- [6] D. Zelenchuk *et al.*, "W-band planar wide-angle scanning antenna architecture," *J. Infr. Millim. Terahertz Waves*, vol. 34, no. 2, pp. 127–139, Feb. 2013.
- [7] D. R. Jackson and A. A. Oliner, *Leaky-Wave Antennas*. Hoboken, NJ, USA: Wiley, 2007.
- [8] U. Kotthaus and B. Vowinkel, "Investigation of planar antennas for submillimeter receivers," *IEEE Trans. Microw. Theory Techn.*, vol. 37, no. 2, pp. 375–380, Feb. 1989.
- [9] K. S. Yngvesson, T. L. Korzeniowski, Y. S. Kim, E. L. Kollberg, and J. F. Johansson, "The tapered slot antenna-a new integrated element for millimeter-wave applications," *IEEE Trans. Mobile Comput.*, vol. 37, no. 2, pp. 365–374, Feb. 1989.
- [10] V. Nalbandian and C. S. Lee, "Tapered leaky-wave ultrawide-band microstrip antenna," in *Proc. IEEE Int. Symp. Antennas Propag.*, vol. 2, Jul. 1999, pp. 1236–1239.
- [11] W. Hong, T.-L. Chen, C.-Y. Chang, J. W. Sheen, and Y.-D. Lin, "Broadband tapered microstrip leaky-wave antenna," *IEEE Trans. Antennas Propag.*, vol. 51, no. 8, pp. 1922–1928, Aug. 2003.
- [12] N. Nguyen-Trong, T. Kaufmann, and C. Fumeaux, "A wideband omnidirectional horizontally polarized traveling-wave antenna based on half-mode substrate integrated waveguide," *IEEE Antennas Wireless Propag. Lett.*, vol. 12, pp. 682–685, 2013.
- [13] N. Nguyen-Trong, T. Kaufmann, and C. Fumeaux, "A semi-analytical solution of a tapered half-mode substrate-integrated waveguide with application to rapid antenna optimization," *IEEE Trans. Antennas Propag.*, vol. 62, no. 6, pp. 3189–3200, Jun. 2014.
- [14] N. Nguyen-Trong, L. Hall, T. Kaufmann, and C. Fumeaux, "Wideband millimeter-wave antennas with magnetic-dipole patterns integrated in metallic structures," *IEEE Trans. Antennas Propag.*, vol. 64, no. 11, pp. 4877–4882, Nov. 2016.
- [15] A. J. Martínez-Ros, J. L. Gómez-Tornero, and G. Goussetis, "Holographic pattern synthesis with modulated substrate integrated waveguide line-source leaky-wave antennas," *IEEE Trans. Antennas Propag.*, vol. 61, no. 7, pp. 3466–3474, Jul. 2013.
- [16] P. Burghignoli, F. Frezza, A. Galli, and G. Schettini, "Synthesis of broad-beam patterns through leaky-wave antennas with rectilinear geometry," *IEEE Antennas Wireless Propag. Lett.*, vol. 2, no. 1, pp. 136–139, 2003.
- [17] J. L. Gómez-Tornero, A. R. Weily, and Y. J. Guo, "Rectilinear leaky-wave antennas with broad beam patterns using hybrid printed-circuit waveguides," *IEEE Trans. Antennas Propag.*, vol. 59, no. 11, pp. 3999–4007, Nov. 2011.
- [18] J. L. Gómez-Tornero, A. Martínez-Ros, A. Álvarez-Melcón, F. Mesa, and F. Medina, "Substrate integrated waveguide leaky-wave antenna with reduced beam squint," in *Proc. Eur. Microw. Conf.*, Oct. 2013, pp. 491–494.
- [19] J. L. Gómez-Tornero, M. Poveda-García, R. Guzmán-Quirós, and D. Cañete-Rebaque, "Reducing the beam squint in scanned leaky-wave antennas using coupled SIW cavities," in *Proc. IEEE Int. Symp. Antennas Propag. (APSURSI)*, Jun. 2016, pp. 77–78.
- [20] N. Nasimuddin, Z. N. Chen, and X. Qing, "Substrate integrated metamaterial-based leaky-wave antenna with improved boresight radiation bandwidth," *IEEE Trans. Antennas Propag.*, vol. 61, no. 7, pp. 3451–3457, Jul. 2013.
- [21] A. Shahvarpour, A. A. Melcon, and C. Caloz, "Bandwidth enhancement and beam squint reduction of leaky modes in a uniaxially anisotropic meta-substrate," in *Proc. IEEE Int. Symp. Antennas Propag.*, Jul. 2010, pp. 1–4.
- [22] A. Porokhnyuk, T. Ueda, Y. Kado, and T. Itoh, "Nonreciprocal metamaterial for non-squinting leaky-wave antenna with enhanced beam steering," in *Proc. IEEE Int. Symp. Antennas Propag.*, Jul. 2013, pp. 2289–2290.
- [23] H. Mirzaei and G. V. Eleftheriades, "An active artificial transmission line for squint-free series-fed antenna array applications," in *Proc. Eur. Microw. Conf.*, Oct. 2011, pp. 503–506.
- [24] H. Mirzaei and G. V. Eleftheriades, "Arbitrary-angle squint-free beam-forming in series-fed antenna arrays using non-Foster elements synthesized by negative-group-delay networks," *IEEE Trans. Antennas Propag.*, vol. 63, no. 5, pp. 1997–2010, May 2015.
- [25] A. Neto, S. Bruni, G. Gerini, and M. Sabbadini, "The leaky lens: A broad-band fixed-beam leaky-wave antenna," *IEEE Trans. Antennas Propag.*, vol. 53, no. 10, pp. 3240–3246, Oct. 2005.
- [26] A. Neto, "UWB, non dispersive radiation from the planarly fed leaky lens antenna—Part 1: Theory and design," *IEEE Trans. Antennas Propag.*, vol. 58, no. 7, pp. 2238–2247, Jul. 2010.
- [27] A. Mehdiour, J. W. Wong, and G. V. Eleftheriades, "Beam-squint reduction of leaky-wave antennas using huygens metasurfaces," *IEEE Trans. Antennas Propag.*, vol. 63, no. 3, pp. 978–992, Mar. 2015.

- [28] D. Deslandes and K. Wu, "Substrate integrated waveguide leaky-wave antenna: Concept and design considerations," in *Proc. Asia-Pacific Microw. Conf. (APMC)*, 2005, pp. 346–349.
- [29] A. J. Martinez-Ros, J. L. Gomez-Tornero, and G. Goussetis, "Planar leaky-wave antenna with flexible control of the complex propagation constant," *IEEE Trans. Antennas Propag.*, vol. 60, no. 3, pp. 1625–1630, Mar. 2012.
- [30] O. Quevedo-Teruel, "Controlled radiation from dielectric slabs over spoof surface plasmon waveguides," *Prog. Electromagn. Res.*, vol. 140, no. 4, pp. 169–179, 2013.
- [31] L. Wang, M. Esquius-Morote, H. Qi, X. Yin, and J. R. Mosig, "Phase corrected *H*-plane horn antenna in gap SIW technology," *IEEE Trans. Antennas Propag.*, vol. 65, no. 1, pp. 347–353, Jan. 2017.
- [32] L. Wang, M. Garcia-Vigueras, M. Alvarez-Folgueiras, and J. R. Mosig, "Wideband *H*-plane dielectric horn antenna," *IET Microw. Antennas Propag.*, vol. 11, no. 12, pp. 1695–1701, Oct. 2017.



**Lei Wang** (S'09–M'16) was born in Nanjing, China, in 1986. He received the B.S. degree in applied physics from the Nanjing University of Posts and Telecommunications, Nanjing, in 2009, and the Ph.D. degree in electromagnetic field and microwave technology from Southeast University, Nanjing, in 2015.

From 2014 to 2016, he was a Research Fellow and held a post-doctoral position with the Laboratory of Electromagnetics and Antennas, Swiss Federal Institute of Technology, Lausanne, Switzerland. From 2016 to 2017, he was a Post-Doctoral Research Fellow with the Electromagnetic Engineering Laboratory, KTH Royal Institute of Technology, Stockholm, Sweden. Since 2017, he has been an Alexander von Humboldt Fellow with the Institute of Electromagnetic Theory, Hamburg University of Technology, Hamburg, Germany. His current research interests include the antenna theory and applications, active electronically scanning arrays, integrated antennas and arrays, substrate-integrated waveguide antennas, leaky-wave antennas, horn antennas, and numerical modeling and optimization of small antennas, microwave frontends, and systems.

Dr. Wang was the recipient of the Chinese National Scholarship for Ph.D. Candidates by the Chinese Government in 2014. He was also the recipient of the Swiss Government Excellence Scholarship of the Swiss Government to conduct research on SIW horn antennas and applications in 2014 and the Alexander von Humboldt Research Scholarship of the German Government to take research on antenna modeling and optimization in 2016. He was the recipient of the Best Poster Award from the 2018 IEEE International Workshop on Antenna Technology.



**José Luis Gómez-Tornero** (S'01–M'06–SM'14) was born in Murcia, Spain, in 1977. He received the degree in telecommunications engineering from the Polytechnic University of Valencia, Valencia, Spain, in 2001, and the Laurea (Ph.D.) degree (*cum laude*) in telecommunication engineering from the Technical University of Cartagena (UPCT), Cartagena, Spain, in 2005.

In 2000, he joined the Radio Frequency Division, Industry Alcatel Espacio, Madrid, Spain, where he was involved in the development of microwave active circuits for telemetry, tracking, and control transponders for space applications. In 2001, he joined UPCT, where he has been an Associate Professor since 2008. He was the Vice Dean for Students and Lectures affairs as a member of the Telecommunication Engineering Faculty, UPCT. He has been a Visiting Researcher/Professor with the University of Loughborough, Loughborough, U.K., Heriot-Watt University, Edinburgh, U.K., the Queen's University of Belfast, Belfast, U.K., and the CSIRO-ICT Center, Sydney, NSW, Australia. In 2010, he was appointed as a CSIRO Distinguished Visiting Scientist with the CSIRO ICT Center. He has co-authored over 50 peer-reviewed journal papers and over 100 conference papers. His current research interests include the development of numerical methods for the analysis and design of leaky-wave devices in planar and waveguide technologies; their application for telecoms, RF identification/localization, microwave heating/sensing, wireless power transmission/harvesting, hyperthermia, and analog signal processing; and the innovation in the area of higher education teaching/learning.

Dr. Gómez-Tornero was a recipient of the National Award from the foundation EPSON-Ibrica for the best Ph.D. project in technology of information and communications in 2004 and the Vodafone Foundation Award for the best Spanish Ph.D. thesis in advanced mobile communications technologies in 2006. His thesis also received the Best Thesis Award in electrical engineering from UPCT in 2006. His Ph.D. students' theses have received the 2014 Hispasat Prize and the 2015 Hisdesat Prize for the best Ph.D. thesis in satellite communication technologies. He was a co-recipient of the 2010 IEEE Engineering Education Conference Award, the 2011 EuCAP Best Student Paper Prize, the 2012 EuCAP Best Antenna Theory Paper Prize, the 2012 and 2013 Spanish URSI Prize for the best student paper, and the 2018 iWAT Best Poster Award.



**Oscar Quevedo-Teruel** (M'10–SM'17) received the M.Sc. degree in telecommunication engineering from the Carlos III University of Madrid, Madrid, Spain, in 2005, the M.E. degree from the Chalmers University of Technology, Gothenburg, Sweden, and the Ph.D. degree from the Carlos III University of Madrid in 2010.

He was then held a post-doctoral research position with the Delft University of Technology, Delft, The Netherlands. From 2010 to 2011, he was with the Department of Theoretical Physics of Condensed Matter, Universidad Autonoma de Madrid, Madrid, as a Research Fellow and went on to continue his post-doctoral research with the Queen Mary University of London, London, U.K., from 2011 to 2013. In 2014, he joined the School of Electrical Engineering/Electromagnetic Engineering, KTH Royal Institute of Technology, Stockholm, Sweden, where he is currently an Associate Professor. He has co-authored over 50 papers in international journals and over 100 papers at international conferences. He holds two patents. His current research interests include microstrip patch antennas, lens antennas, metasurfaces with higher symmetries, transformation optics, and high-impedance surfaces.